

Supplementary Materials for **Survival of spin state in magnetic porphyrins contacted by graphene nanoribbons**

Jingcheng Li, Nestor Merino-Díez, Eduard Carbonell-Sanromà, Manuel Vilas-Varela, Dimas G. de Oteyza, Diego Peña, Martina Corso, Jose Ignacio Pascual

Published 16 February 2018, *Sci. Adv.* **4**, eaq0582 (2018)
DOI: 10.1126/sciadv.aq0582

This PDF file includes:

- note S1. Symmetry of fused FeTPP moieties
- note S2. Spectra on pyrrole subunits of GNR-contacted FeTPPs
- note S3. Anomalous contacts between FeTPP and GNRs
- note S4. Electronic structure of contacted FeTPPs
- fig. S1. Statistics of different types of FeTPP connected to cGNRs.
- fig. S2. dI/dV spectra taken over the pyrrole subunits of cGNR-contacted FeTPP moieties.
- fig. S3. Additional bond formation between planar FeTPP and cGNRs.
- fig. S4. Comparison of wide-range dI/dV spectra on pristine and on contacted FeTPP.
- fig. S5. Frontier orbitals of FeTPP and their localization in the macrocycle.

note S1. Symmetry of fused FeTPP moieties

As we mentioned in the main text, to fully complete the cyclodehydrogenation (CDH) step the substrate was annealed to 250°. This resulted in the additional CDH-fusion of the FeTPP rings to the macrocycle. Such planarization reaction has been widely reported (see e.g. refs. [17,21,22] in the manuscript). In the fig. S1b we show that after preparation at this annealing temperature only 5% of the FeTPP molecules remained with the original saddle shape (not-fused), whereas 80% appeared with all the phenyl rings fused to the macrocycle, and the rest only partly fused. Preparing at a lower temperature did change these fractions, but the cGNRs were not fully formed.

Since each phenyl of the FeTPP moiety can fuse either clockwise or anticlockwise, the fused structures can be of four different types, each with a different symmetry. We show in the fig. S1a the structure of these four types, labeled C4-symmetric, Mirror-symmetric 1, Mirror-symmetric 2, and Asymmetric [22]. The structure of the contacted FeTPP moieties was characterized by high resolution images with a CO-terminated tip, as shown in the main manuscript. Contrary to the expected statistical fraction of each structure (1/8, 2/8, 1/8, and 3/8, respectively), we find that the most frequently found species correspond to C4-symmetry and to Asymmetric types (see fig. S1c), while planar FeTPPs with mirror symmetry was rarely found.

These results clearly differ from planarization reaction of metal-TPPs [22], indicating that the contact to GNRs plays an important role in the way the planarization proceeds. We speculate that, since cGNRs are more extended structures than the porphyrin, the fusion takes most probably place by a rotation of the porphyrin macrocycle respect to the less mobile cGNRs. In this way, we explain that the phenyl rings of a planar FeTPP show the tendency to appear fused in the same orientation.

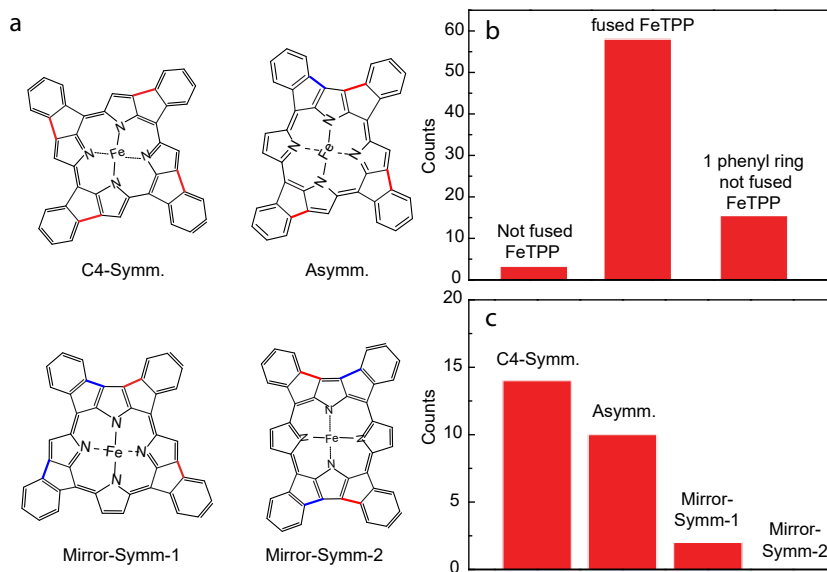


fig. S1. Statistics of different types of FeTPP connected to cGNRs. **a**, Structure of the four possible configurations of FeTPP moieties expected after planarization. **b**, Bar plot of the number of saddle FeTPP, fused FeTPP, and FeTPP with 1 phenyl ring not fused. **c**, Bar plot of the number of planar FeTPP moieties found with the structure of panel **a**.

note S2. Spectra on pyrrole subunits of GNR-contacted FeTPPs

The main text focus on dI/dV spectra taken over the iron centers of different types of FeTPP moieties connected to cGNRs. These spectra show spin excitation features. Here, we show similar spectra taken over the pyrrole units of the FeTPP. Figure S3a-d picture the FeTPP moieties of the hybrids shown in Fig. 2a, Fig. 3a, Fig. 4a,b in the main text, respectively. For the saddle (non-planar) FeTPP, the spin excitation spectra is only observed on the two upwards pyrrole subunits (fig. S2e), as observed in pristine FeTPP molecules [16]. For all planar FeTPP species, clear inelastic features are observed over all (fused) pyrroles. The corresponding excitation energy value obtained from the spectra shown in fig. S2e are summarized in fig. S2f. The excitation energies for each configuration are estimated from the bias value at the middle of the step. Even for the narrower features (plots 8-10 in fig. S2e) the narrow dip can be ascribed to spin excitation: their asymmetric shape is caused from particle-hole asymmetry, as shown in ref. [30]. The general trend observed over the pyrroles coincide with the results shown in Fig. 4f in the main manuscript.

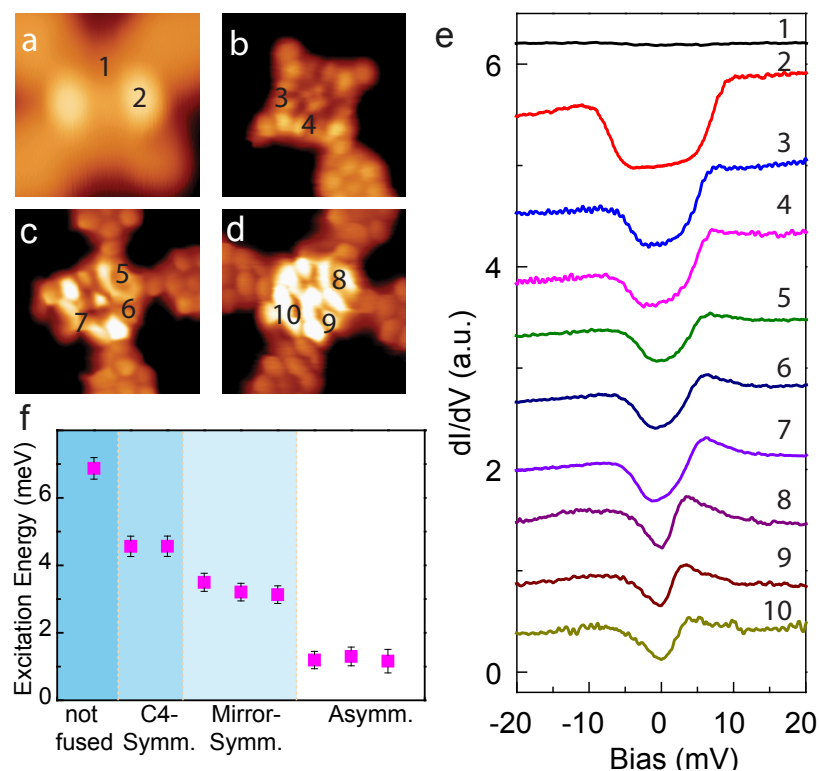


fig. S2. dI/dV spectra taken over the pyrrole subunits of GNR-contacted FeTPP moieties. **a-d**, STM images of the FeTPP parts of devices shown in Fig. 2a, Fig. 3a, Fig. 4a,b of the main text, respectively. **e**, dI/dV spectra taken over pyrrole units indicated with numbers in **a-d** ($V_s = 50$ mV, $I_t = 1$ nA, modulation voltage $V_{ac} = 0.4$ mV rms). **f**, Excitation energy values obtained from fits to spectra in **e**. The data points from left to right are corresponding to the spectra 2 to 10 respectively.

note S3. Anomalous contacts between FeTPP and GNRs

Apart from the structures shown in the main text, a few hybrid systems show additional C-C bonds connecting the cGNR termination with the FeTPP macrocycle. Figure S3a,b shows two of such systems for a fused-FeTPP with asymmetric configuration. In these cases, spectra taken over the iron center show no spin excitation features. These results thus suggest that deviations from the atomically precise contact structure might result in complete removal of the functionality of the active element.

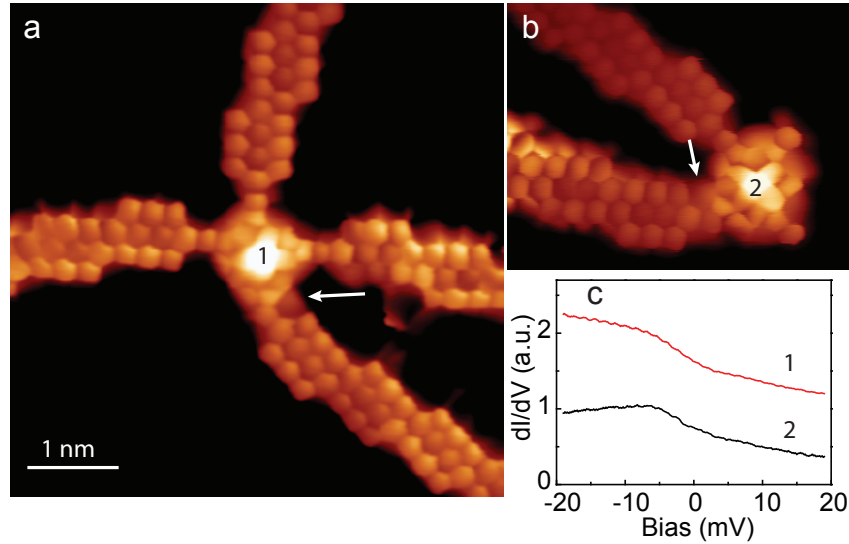


fig. S3. Additional bond formation between planar FeTPP and cGNRs. **a,b**, constant height dI/dV maps of an asymmetric planar-FeTPP obtained with a CO terminated tip ($V_S = 0$ V, $V_{ac} = 2$ mV, $R_t \sim 1$ G Ω). The white arrows indicate the additional bond created at the junction between FeTPP and cGNRs. All images share the same scale bar. **c**, dI/dV spectra taken on the central Fe atoms of structures in **a** and **b** ($R_t = 50$ M Ω , $V_{ac} = 0.4$ mV). The dI/dV spectra are vertically shifted for clarity.

note S4. Electronic structure of contacted FeTPPs

In fig. S4 we compare the electronic structure of saddle-FeTPP and C4-planarized FeTPP species with that of pristine FeTPP on Au(111) [16]. The pristine molecule shows several broad resonances around zero bias, with rising conductance towards negative bias. Results from DFT simulations [16] found that these correspond to the manifold of spin-polarized d - resonances of the Fe ion, with majority character stemming from d_{z^2} and d_{xy} orbitals, which dominates the density of states (DOS) over the Fe ion around the Fermi level. The spectra on cGNR-contacted saddle FeTPP shows identical features, thus corroborating that the electronic structure of the porphyrin in the hybrid is not affected. The C4-planarized FeTPP shows a similar set of spectral features around and below E_F , what allows us to associate it with the d -manifold in Fig. 5 of the main manuscript.

Over the organic corolla, three clear molecular resonances appeared over the protruding pyrroles in the pristine species. In particular, a state lying approximately at 150 meV above E_F (the LUMO) was attributed to a molecular orbital composed of pyrrole states and empty d_{yz} components of the Fe ion, having a strong hybrid Fe-ligand character and spin polarization. As we show in fig. S4b, this state survives in the contacted porphyrins.

Figure S5a studies the LUMO resonance in more detail and its distribution along the molecular axis of a saddle FeTPP contacted to cGNRs. Over the pyrroles the LUMO state is appears at $V_S \sim 120$ mV, while over the Fe^{2+} center, a broader resonant shows at negative

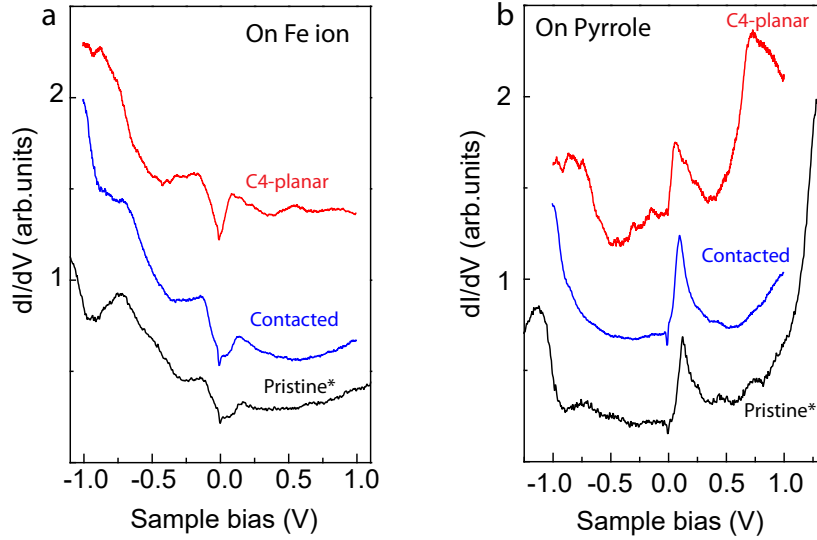


fig. S4. Comparison of wide-range dI/dV spectra on pristine and on contacted FeTPP. Wide range dI/dV spectra taken **a** over the Fe^{2+} center, and **b** over a pyrrole site, of a pristine (bottom), saddle (middle), and C4-symmetric (top) planar FeTPP. (*) We acknowledge C. Rubio for providing the data for the pristine species as a reference [16]. The agreement with results from ref. [16] allows us to identify the frontier molecular resonances as states with either Fe d character, on the center, or Fe d_{yz} character, on the upper pyrroles.

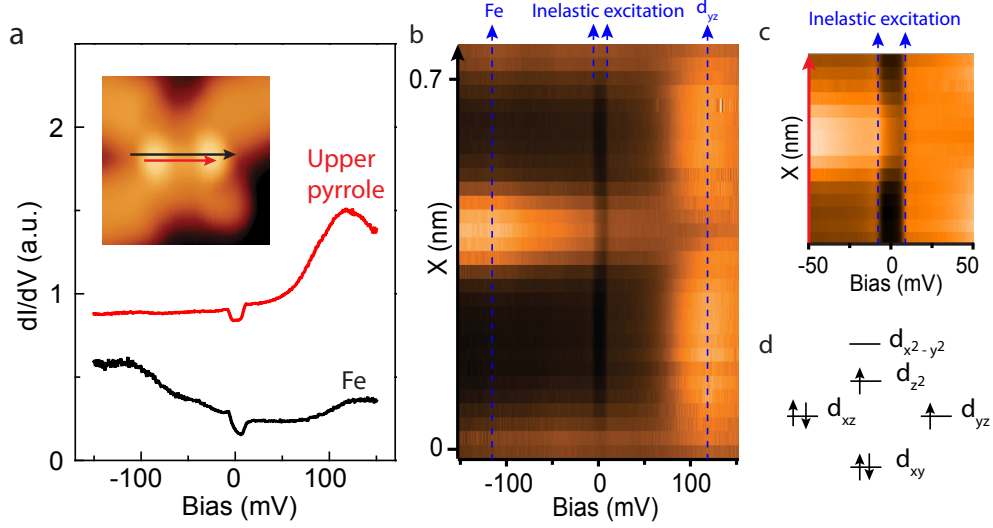


fig. S5. Frontier orbitals of FeTPP and their localization in the macrocycle. **a**, dI/dV spectra taken on the upper pyrrole and on the Fe^{2+} center of a saddle (non-fused) FeTPP shown in the inset ($R_t \sim 150 \text{ M}\Omega$, $V_{ac} = 4 \text{ mV rms}$). **b,c**, Spectral map along the molecular axis in wider range and narrow range (black and red arrow in the inset of panel **a** respectively). The agreement with results from ref. [16] allows us to identify the frontier molecular resonances as states with either Fe d character, on the center, or Fe d_{yz} character, on the upper pyrroles. **c**, Scheme of the orbital occupation, obtained from ref. [16].

bias. Figure S5b shows a spectral map of dI/dV vs. V_S along the axis of the molecule, capturing the peculiar localization of the two frontier states within the macrocycle structure. In both figures the inelastic features around zero bias are easily detected. These results coincide with findings in ref. [16], where the spin configuration of FeTPP was found to be $S=1$, with easy plane anisotropy constant $D \sim 7 \text{ meV}$, and with orbital filling as depicted in fig. S5c. Hence, the magnetic properties of cGNR-contacted FeTPP are identical to pristine FeTPP.